Ecological Modelling 246 (2012) 1–10

Contents lists available at SciVerse ScienceDirect

Ecological Modelling

journal homepage: www.elsevier.com/locate/ecolmodel

Effect of population size in a predator–prey model

F. Campillo*, C. Lobry

Modemic Team-Project INRA/INRIA, SupAgro, 2 Place Viala, 34060 Montpellier Cedex 2, France

ARTICLE INFO

Article history:
Received 1 December 2011
Received in revised form 1 July 2012
Accepted 3 July 2012

Keywords:
Predator–prey model
Ordinary differential equations
Diffusion equations
Gillespie algorithm
Birth and death processes

ABSTRACT

We consider a hybrid version of the basic predator–prey differential equation model: a pure jump stochastic model for the prey variable x coupled with a differential equation model for the predator variable y. This hybrid model is derived from the classical birth and death process. The model contains a parameter ω which represents the number of individuals for one unit of prey: $x = 1$ corresponds to ω individual prey. It is shown by the mean of simulations and explained by a mathematical analysis based on a result from the *singular perturbation theory* – the so-called theory of *Canards* – that qualitative properties of the model like persistence or extinction are dramatically sensitive to ω. For instance, in our example, if $\omega = 10^7$ we have extinction and if $\omega = 10^8$ we have persistence. This means that we must be very cautious when we use continuous variables in place of discrete ones in dynamic population modeling even when we use stochastic differential equations in place of deterministic ones.

1. Introduction

Consider the standard predator–prey model:

$$\begin{cases} \dfrac{dx}{dt} = f(x) - \mu(x)y, \\ \dfrac{dy}{dt} = (c\,\mu(x) - \delta)y \end{cases} \tag{1}$$

where x stands for the concentration of prey and y for the concentration of predators. It is well-known that this kind of modeling with differential equations is valid only if *one unit* of both x and y represents a *large number* of both predator and prey *individuals*.

It has long been known that only stochastic models with discrete values are brought to account for such dynamics when population sizes are small. Indeed, in his 1939 article where William Feller introduced birth and death processes as an example of continuous time Markov processes with discrete state space, he immediately applied them to the modeling of population dynamics including the Lotka–Volterra dynamics (Feller, 1939). Several studies have pursued the analysis of Lotka–Volterra type stochastic processes, in the form of birth and death processes (Bartlett, 1957; Leslie, 1958) but also of diffusion processes (Gard and Kannan, 1976). In particular, since Bartlett (1957) it is known that the treatment of extinction is radically different in deterministic and stochastic models; in the latter case the demographic noise leads to predator species extinction in finite time.

More recently, Daniel Gillespie independently published a famous paper about the exact Monte Carlo simulation of such birth and death processes within the framework of chemical kinetics (Gillespie, 1977). Our present work was partly inspired by the latter work. Even more recently, the question of the inadequacy of deterministic continuous modeling is firmly addressed in Mollison (1991) that criticizes the biological interpretations of Murray et al. (1986). Let us quote from Mollison (1991):

> *As to the second wave, close inspection shows that the explanation lies not much in the determinism of the model as in its modeling of the population as continuous rather than discrete and its associated inability to let population variables reach the value zero. Thus the density of infected at the place of origin of the epidemic never becomes zero; it only declines to a minimum of around one atto-fox (10^{-18} of a fox, cf. R. Hughes "The Fox in the Attic", Chatto & Windus, London, 1961) per square kilometer. The model then allows this atto-fox to start the second wave as soon as the susceptible population has regrown sufficiently.*

What is meant by *large* is generally not specified but it is widely admitted that at around 10^3 the law of large numbers begins to be effective and that figures such as 10^6 allow the use of continuous variables and differential equations.

The objective of this article is to show that the threshold of 10^3 is not always acceptable and that, in some circumstances, even 10^6 cannot be considered as secure when we deduce biological consequences, such as persistence, from the behavior of a model with continuous variables. For this purpose we analyze a stochastic model such that the dynamic of the process is locally approximated, when the number of prey is large, by a differential system, which is precisely a predator–prey model of type (1). We agree

* Corresponding author.
E-mail address: Fabien.Campillo@inria.fr (F. Campillo).

0304-3800/$ – see front matter © 2012 Elsevier B.V. All rights reserved.
http://dx.doi.org/10.1016/j.ecolmodel.2012.07.015

that in many respects, our model is biologically questionable but our objective is not to contribute to the biological understanding of the predator–prey relationship. Our objective is rather to point out a mathematical phenomenon, which is likely to be present in many models and that might be responsible for erroneous interpretations.

Except in Turner (2007), which is mathematically oriented, we are not aware of papers describing this phenomenon in dynamical population literature.

The first section is devoted to the presentation of the model, the second to the presentation of some unforeseen simulations, the third to the analysis of the differential system and the fourth to an explanation of the unexpected aspects of the simulations. The last sections is devoted to methodological comments.

A key point in our explanation relies on the fact that the continuous system approximating the model is a so-called "slow-fast" system which exhibits a "canard solution". "Canard solution" is now well-known among specialists of singular perturbation theory of differential equations, see for instance the recent review Desroches et al. (2012). For the the convenience of the interested reader we have written a short appendix on this question.

From the mathematical point of view the material and results presented here are classical. The article is intended principally for non mathematically oriented readers who are not necessarily aware of these questions. We have tried to avoid all mathematical technicalities and for this purpose we have made extensive use of computer simulations.

2. The model

We built a stochastic model which is approximated, in a sense that will be made precise later, by the system of differential equations:

$$\begin{cases} \dfrac{dx}{dt} = \dfrac{1}{\varepsilon}[f(x) - \mu(x)y], \\ \dfrac{dy}{dt} = (\mu(x) - m)y \end{cases} \tag{2}$$

which is, after a change of unit time, the classical deterministic differential predator–prey model (1) with $c = \varepsilon$, $\varepsilon m = \delta$.

The variable $\omega x(t)$ is an integer which is the number of prey at time t. This variable performs the following birth and death process (here "death" means "capture" by a predator):

- At any time, the epoch τ of the next event (birth or death) is a random variable Z which follows an exponential distribution law of parameter:

$$\lambda = \frac{\omega}{\varepsilon}(f(x) + \mu(x)y). \tag{3a}$$

- At the epoch τ we have one birth with probability $\frac{f(x)}{f(x)+\mu(x)y}$ or one death with the complementary probability, that is:

$$\begin{aligned} \mathbb{P}(\omega x(\tau^+) = \omega x(\tau^-) + 1) &= \frac{f(x(\tau^-))}{f(x(\tau^-)) + \mu(x(\tau^-))y(\tau^-)}, \\ \mathbb{P}(\omega x(\tau^+) = \omega x(\tau^-) - 1) &= \frac{\mu(x(\tau^-))y(\tau^-)}{f(x(\tau^-)) + \mu(x(\tau^-))y(\tau^-)}. \end{aligned} \tag{3b}$$

The variable y is a continuous variable which evolves according to:

$$y(t + dt) = y(t) - dt\, m\, y(t) + \varepsilon \times \{\text{number of captures during } [t, t + dt]\}. \tag{3c}$$

Thus the predator dynamics is an exponential decay associated to a growth proportional to the number of prey disappearing during the elapsed time. The parameter ε accounts for different time scales for the predator and prey dynamics.

It might seem curious to have a discrete model for the evolution of the prey and a continuous one for the predator since, in many cases, the density of prey is much larger than the density of predators. But it is not always the case, for instance viruses, which have a far more higher density are predators of bacteria.

Assume that $dt = 10^{-4}$, $\omega = 10^9$, $\varepsilon = 10^{-1}$ and $f(x) + \mu(x)y$ is of the order of the unit. Then, during an elapsed time of dt the number of events, death or birth, is of the order of $\lambda\, dt = \frac{\omega}{\varepsilon}(f(x) + \mu(x)y)dt \approx \frac{10^5}{\varepsilon} \approx 10^6$. This is somewhat lengthy to simulate, at least with a desk computer, but due to this large number of events, the process defined by (3) is accurately approximated on the interval $[t, t + dt]$ by the following diffusion process whose derivation is presented in Appendix A:

$$\begin{cases} x(t + dt) = x(t) + \dfrac{dt}{\varepsilon}[f(x(t)) - \mu(x(t))y(t)] - \sigma_x W_t, \\ y(t + dt) = y(t) + dt[(\mu(x(t)) - m)y(t)] + \sigma_y W_t \end{cases} \tag{4}$$

where $W_{1dt}, W_{2dt}, W_{3dt}, \ldots$ is a sequence of independent Gaussian variables with mean 0 and standard deviation 1, and:

$$\sigma_x = \sqrt{\frac{4\,dt}{\omega\,\varepsilon}}\sqrt{\frac{f(x(t))\mu(x(t))y(t)}{f(x(t)) + \mu(x(t))y(t)}},$$
$$\sigma_y = \sqrt{\frac{dt\,\varepsilon}{\omega}}\sqrt{\frac{f(x(t))\,\mu(x(t))y(t)}{f(x(t)) + \mu(x(t))y(t)}}.$$

This diffusion approximation is not valid for small x, in this case one must switch to the pure jump process. As we do not aim to focus on small x, we restrict ourselves to the consideration of the stochastic diffusion like process with continuous variables:

$$\begin{cases} \text{if } x(t) \le \dfrac{1}{\omega} \text{ then } x(t + dt) = 0 \text{ else} \\ x(t + dt) = x(t) + \dfrac{dt}{\varepsilon}[f(x(t)) - \mu(x(t))y(t)] + \sigma_x W_t \\ y(t + dt) = y(t) + dt[(\mu(x(t)) - m)y(t)] + \sigma_y W_t \end{cases} \tag{5}$$

The first line in (5) states that when the number of prey is smaller than 1 it has to be 0. This needs to be specified as the variable x in the diffusion model is now continuous but still we want to keep the meaning of x as a *number of individuals*. Thus, $\frac{1}{\omega}$ must be an absorbing barrier for (5). For $x \ge \frac{1}{\omega}$ one sees that the recurrence equation for the mean of $x(t)$ and $y(t)$ is approximated by:

$$\begin{cases} \mathbb{E}[x(t + dt)] = \mathbb{E}[x(t)] + \dfrac{dt}{\varepsilon}[f(x(t)) - \mu(x(t))y(t)] \\ \mathbb{E}[y(t + dt)] = \mathbb{E}[y(t)] + dt[(\mu(x(t) - m)y(t)] \end{cases} \tag{6}$$

which is precisely the Euler scheme for the differential system (2).

To summarize this section, we have constructed a diffusion model (5) which depends on a parameter ω. This model has the following properties:

- Since the model is derived from a birth and death process, x units of prey correspond to ωx individuals.
- The standard deviation is proportional to $\sqrt{\frac{1}{\omega}}$: the larger ω is the more "deterministic" the process.
- The diffusion process is degenerate, i.e. the dimension of the random noise is not 2 but 1. This is due to the fact that only x is considered as a discrete variable, not y.
- When ωx is large, greater than 10^3, the dynamic of the mean is accurately approximated, at least for small durations, by the classical deterministic differential predator–prey model (2).

We shall first simulate this system and then explain the observed simulations.

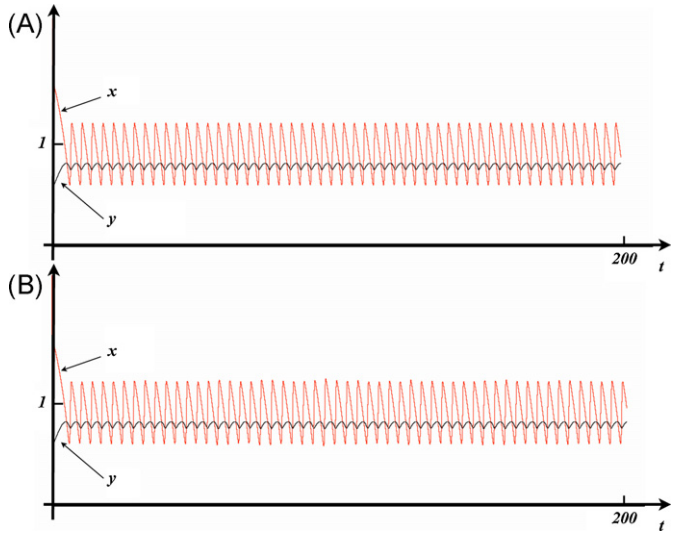

Fig. 1. Two runs of the process (5): population of prey in red, predator in black; (A) for $\omega = 10^{12}$; (B) for $\omega = 10^{10}$. No difference is visible: the two processes perform stable oscillations. (For interpretation of the references to color in this figure legend, the reader is referred to the web version of this article.)

3. Simulations

In this section we fix $f(x) = \frac{1}{2}x(2-x)$, $\mu(x) = \frac{x}{0.4+x}$, $\varepsilon = 0.02$ and $m = 0.6645$. For a duration of 200, two runs of the process (5) are plotted in Fig. 1: one for $\omega = 10^{12}$ (A) and one for $\omega = 10^{10}$ (B). One sees regular oscillations for the population of prey (in red) and predator (in black). We do not see any difference between the two runs. These regular oscillations are those predicted by the deterministic predator–prey model. The value of x during the oscillations is around 1, which corresponds to a large number of individuals, it is then not surprising that the continuous deterministic system is a good approximation.

But in Fig. 2 we observe a dramatic change when $\omega = 10^8$, *which is still a large figure*. We observe a *mixed mode oscillation* with random successions of large and small oscillations that could not be produced by a deterministic two dimensional system. With $\omega = 10^6$ we

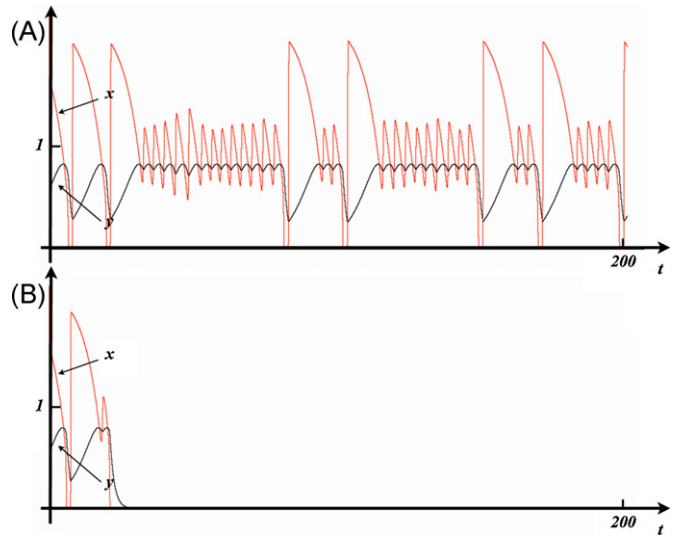

Fig. 2. Two runs of the process (5): population of prey in red, predator in black; (A) for $\omega = 10^8$; (B) for $\omega = 10^6$. For these values of ω the dynamics are very different from those of Fig. 1: oscillations are not stable and lead to extinction. (For interpretation of the references to color in this figure legend, the reader is referred to the web version of this article.)

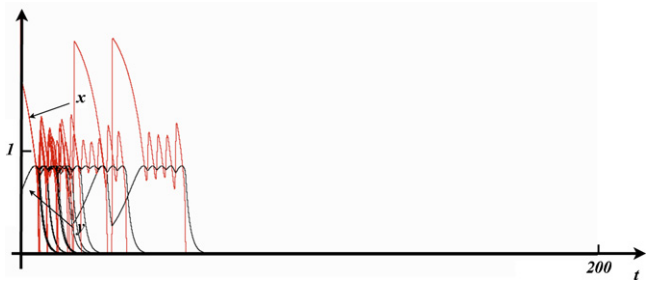

Fig. 3. Twenty independent runs of the process (5) with $\omega = 10^6$, population of prey in red, predator in black. In all runs the two populations goes to extinction. (For interpretation of the references to color in this figure legend, the reader is referred to the web version of this article.)

observe an extinction of the two populations, which is confirmed in Fig. 3 where none of the 20 runs for $\omega = 10^6$ is persistent at time $T = 200$.

Let T denote the time of extinction for the predator, defined as the time when $y(t)$ reaches the value $\frac{1}{\omega}$. Let us say that there is extinction when the time of extinction is smaller than 1000. In Table 1 we have the empirical probabilities of extinction with respect to ω, computed on 1000 runs, and the mean and standard deviation of T, computed on the trajectories ending with extinction for $t < 1000$.

We can see that the transition is very sharp from extinction with probability one ($\omega = 4.0 \times 10^6$) to non extinction with probability one ($\omega = 2.0 \times 10^7$). It seems surprising that at $\omega = 2.0 \times 10^7$ prey individuals and above, the system is persistent but, with still a big figure like $\omega = 4.0 \times 10^6$ and below, the system is definitively not.

This is a problem since in most population dynamics models, we have poor information on the actual size of a population. We shall come back to this issue later. Notice also that the standard deviation of T is very large for small values of ω which makes predictions very imprecise. The explanation of this somewhat unexpected phenomenon is given by the analysis of the associated deterministic model (2).

4. The dynamics of the continuous deterministic model

We now describe the dynamics of the deterministic model (2) that approximate the evolution of the mean of the diffusion model (6). All the material in this section is classical in mathematical literature and known as the theory of "canards", see Appendix B

Table 1
Empirical probabilities of extinction according to ω.

ω	$\mathbb{E}[T]$	$\sigma(T)$	$\mathbb{P}(T \le 1000)$
10^5	30.46	6.75	1
10^6	39.02	11.30	1
2.0×10^6	47.74	19.62	1
4.0×10^6	79.05	51.79	1
6.0×10^6	143.54	121.42	0.999
8.0×10^6	259.76	222.64	0.983
9.0×10^6	311.70	247.58	0.964
1.0×10^7	554.21	319.94	0.867
1.1×10^7	555.17	351.75	0.741
1.2×10^7	681.31	324.12	0.649
1.3×10^7	745.83	321.95	0.481
1.4×10^7	815.46	296.26	0.384
1.5×10^7	867.54	273.60	0.255
1.6×10^7	906.10	238.55	0.182
1.7×10^7	928.68	221.50	0.120
1.8×10^7	964.05	143.82	0.072
1.9×10^7	975.48	110.09	0.059
2.0×10^7	>1000		0

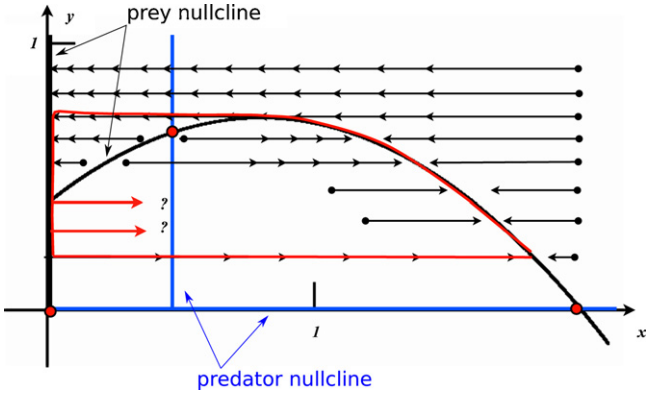

Fig. 4. Schematic representation of solutions of (2) for small value of m. Due to the presence of a small ε, trajectories must be almost horizontal except in the neighborhood of the parabola (see comment in the text).

for more details about this theory and an explanation of the word "canard".

The first step in the understanding of a planar system like ours is to draw the two nullclines, also called "zero growth isoclines", i.e. the sets defined by:

- the nullcline of the prey: $\{(x, y) : \frac{1}{\varepsilon}[f(x) - \mu(x)y] = 0\}$;
- the nullcline of the predator: $\{(x, y) : (\mu(x) - m)y = 0\}$.

In our simulations the parameter ε is small (0.02) and thus, except when the quantity

$$[f(x) - \mu(x)y]$$

is small (of the order of ε), the right member in the first equation in (2) is large compared to the right member in the second equation. This means that the vector velocity of (2) is *almost horizontal*. Hence a first approximation of the solution of our system is shown by the hand-drawn schemes in Figs. 4 and 5: Outside of the parabola and the y-axis, which is the nullcline of the prey, the trajectories are taken as horizontal.

In Fig. 4 one sees that the predator nullcline (in blue) contains a vertical line that intersects the prey nullcline (the black y-axis and the black parabola). The intersection point (the red dot) is on the left of the maximum of the prey nullcline. Along the parabola prey nullcline, the motion is upward on the right of the blue vertical, and downward on the left. From this one sees that the trajectories join the y-axis in an attractive part (above the top of the parabola), then they go down along the y-axis and finally – after crossing the parabola – there is uncertainty about the place the trajectory exits

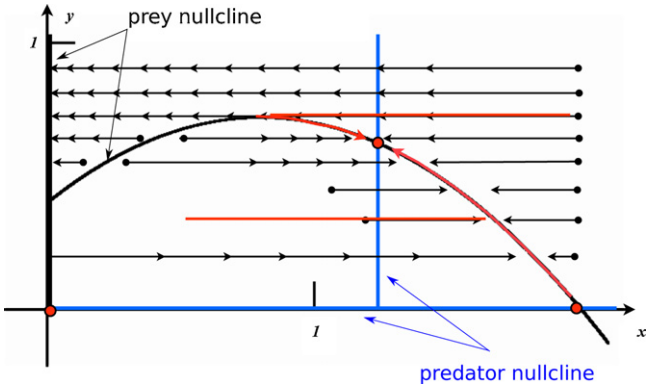

Fig. 5. Schematic representation of solutions of (2) for large value of m (see comment in the text).

the y-axis. From this diagram we suspect the existence of a periodic limit cycle that can in fact be proven.

In Fig. 5 the situation is somewhat easier to understand. As the blue vertical nullcline of the predator is on the right of the maxima of the parabola prey nullcline, the motion along the parabola converges to a limit point, which is apparently a stable attracting point for all initial conditions.

Notice that an attracting equilibrium and an attracting limit cycle are qualitatively different phase portraits and that the transition between the two cases occurs when m crosses the value 0.666... (i.e. when the blue line crosses the parabola at its maximum).

Let us now comment on Fig. 6. The pictures are not hand-drawn schemes but actual simulations with $\varepsilon = 0.02$; we observe the strong similarity between the schemes:

- For $m = 0.6$, the system features one large limit cycle (the direction of the motion is anti-clockwise). If we consider trajectories with initial conditions $x = 2$ and increasing y coordinates: for small enough y-coordinates, the trajectories go horizontally from left to right, then they meet and follow the limit cycle; for large enough y-coordinates, the trajectories go horizontally from right to left, they pass above the maximum of the parabola and meet the y-axis, then they reappear below the limit cycle and rapidly cross horizontally from left to right where they meet the parabola to finally meet the limit cycle. Actually "true" trajectories never meet but, due to the limit of our drawing, they seem to. All trajectories follow for a while the y-axis and then $x(t)$ becomes potentially small.
- For $m = 0.75$, the system features an attracting equilibrium. Some trajectories go directly to the equilibrium, others follow the y-axis.
- For $m = 0.6645$, the system features a small periodic limit cycle circling around the unstable equilibrium that is very close to the periodic orbit. The periodic orbit is far from the y-axis and $x(t)$ is never small, but one sees that near the unstable equilibrium, a very small perturbation leads to a trajectory that follows the y-axis so that $x(t)$ can become small.
- For $m = 0.66442561$, the system features a limit cycle of intermediate size between "large" (meets the y-axis and follows it for a significative amount of time, like for $m = 0.6$) and "small" (remains far from the y-axis, like for $m = 0.6645$); it meets the y-axis for a short period of time. The point is that these specific intermediate cycles called "canard cycles" are obtained for very sharp values for m (8 digits in our case). See Appendix B for information about the mathematical theory of "canards".

Throughout this description we have said that $x(t)$ is potentially small when the trajectory follows the y-axis. *But how small?* A simple way to depict what is going on along this axis is to plot, not $(x(t), y(t))$, but $(\xi(t), y(t))$ with:

$$\xi(t) = \varepsilon \ln(x(t)).$$

This is shown in Figs. 7 and 8. We represent the (x, y) and the (ξ, y) trajectories in the same system of axes; (x, y) trajectories are in red, (ξ, y) are in green and both limit cycles in the two systems of representation are in blue. The two vertical red lines correspond to $x = 10^{-9}$ and 10^{-6} (see Appendix C for an analytical evaluation). There are 19 trajectories starting from $(2, 0.5 \pm k\,0.05)$ $k = 0, 1, \ldots, 9$.

Let us compare the two simulations.

- Fig. 7: We look at the "large" limit cycle in the (ξ, y) variables and we see that the minimum of ξ corresponds to $x = 10^{-9}$; for the

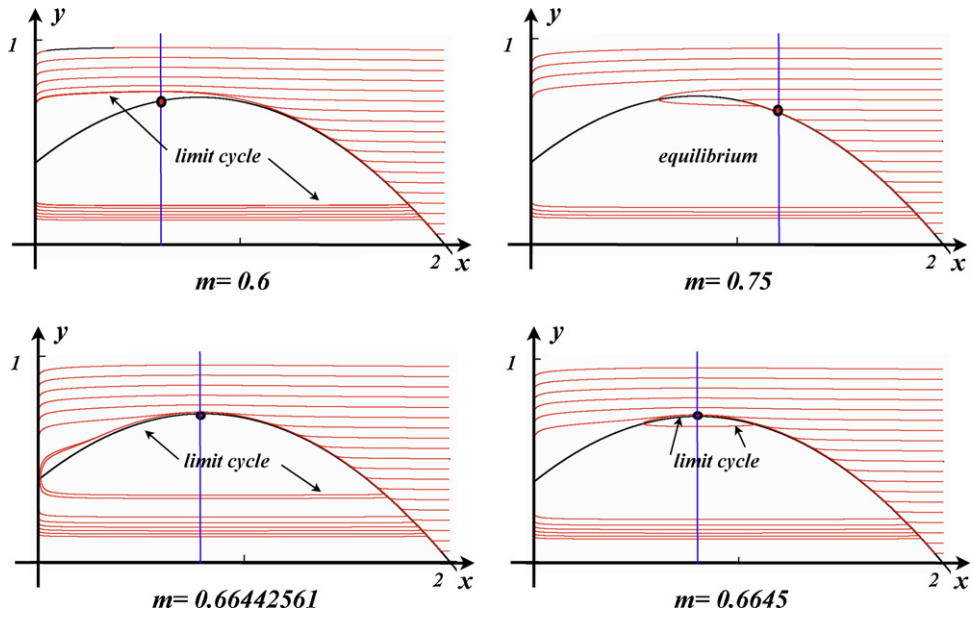

Fig. 6. Computer simulations of the phase portrait of system (2) in red, for different values of m. One sees that the computed solutions are very close to the schematic ones. (For interpretation of the references to color in this figure legend, the reader is referred to the web version of this article.)

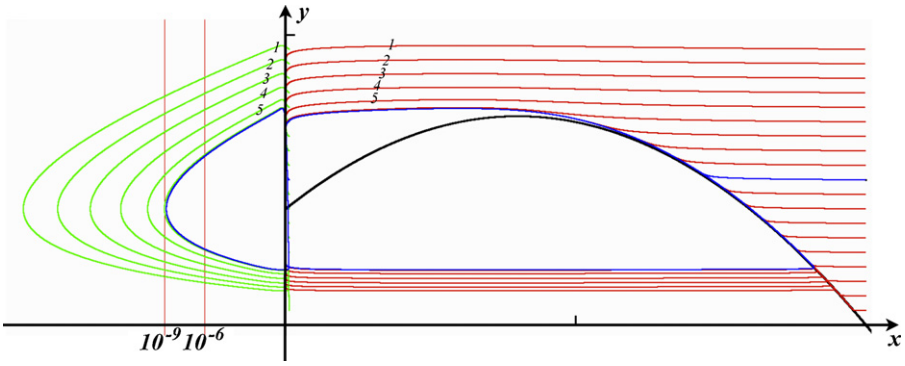

Fig. 7. The trajectories of the system (2) in the (x, y) variables (in red) and in the (ξ, y) variables (in green), i.e. log scale for x, on the same system of axes for $m = 0.6$. When x is very close to the y axe its logarithm is large and negative. (For interpretation of the references to color in this figure legend, the reader is referred to the web version of this article.)

trajectory labeled 1 the minimum is about 10^{-17}. These incredibly small values can be easily explained, see Appendix B.

- Fig. 8: The "small" limit cycle is almost not visible in the (ξ, y) variables. In both the (ξ, y) and the (x, y) variables the trajectories labeled 1 to 4 look very similar. But trajectory 5 remains above 10^{-9}, which is not the case in Fig. 7, and trajectory 6 does not exist in Fig. 7.

The main difference between the case $m = 0.6$ and the case $m = 0.6645$ is that, in the former case each trajectory is such that

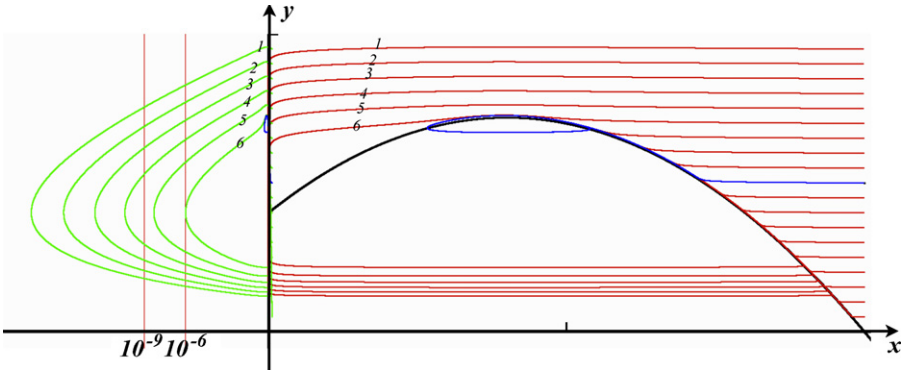

Fig. 8. The trajectories of the system (2) in the (x, y) variables (in red) and in the (ξ, y) variables (in green), i.e. log scale for x, on the same system of axes for $m = 0.6445$. When x is very close to the y axe its logarithm is large and negative. (For interpretation of the references to color in this figure legend, the reader is referred to the web version of this article.)

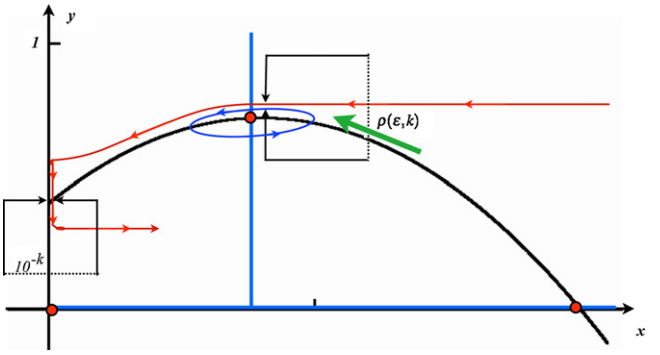

Fig. 9. Schematic representation of the "safety funnel". The trajectory in red is the one for which the minimum of x is 10^k and the limit cycle is in blue. The green arrow shows that trajectories have to go through a very narrow funnel. (For interpretation of the references to color in this figure legend, the reader is referred to the web version of this article.)

the minimum of x is smaller than 10^{-9}, unlike in the latter case where are two sets of trajectories: those that start above trajectory 6, for which the minimum will be smaller than 10^{-6} before reaching the limit cycle, and the others, for which $x(t)$ remains greater than 10^{-6}. Note that this trajectory 6 is in some places very close to the limit cycle.

The observed differences between $m = 0.6$ and $m = 0.6645$ are not specific to these values. In particular the same behavior with two types of trajectories separated by a sharp transition is true for all values of m between $m = 0.66442561$ and $m = 0.6666\ldots$. This behavior is summarized by the "safety funnel", indicated by the green arrow in Fig. 9. We give an explanation for this now. Assume that for some reason we do not pursue a trajectory such that the minimum of $x(t)$ is smaller than $\alpha = 10^{-k}$ (it may be because we think that the size of the population is too low in order to survive or because we want to switch to a different-stochastic-model). The form $\alpha = 10^{-k}$ is by no means essential for α, it is just to emphasize that α is small. There exists a unique y_0 such that the solution issued from (∞, y_0) (in practice 2 is a good infinite value), which we call the "α-safety trajectory", is such that $x(t)$ first decreases and attains a first local minimum equal to 10^{-k}. This is the red trajectory in Fig. 9. When $x(t) \approx \mu^{-1}(m)$ (the blue vertical), the α-safety trajectory will be very close to the limit cycle (the blue trajectory). Let $\rho(\varepsilon, k)$ denote the distance between the two curves; this quantity can be derived from the values of ε and k. The "safety funnel" is the area delimited by the red and the blue curves on the right of the vertical $x = \mu^{-1}(m)$. If a trajectory, even slightly perturbed, enters the funnel, it has a very high probability that its x-component remains greater than 10^{-k}. If not, there is a danger of reaching values smaller than 10^{-k}.

5. The diffusion process in the variables (x, y) and (ξ, y)

In the two simulations shown in Figs. 10 and 11 we have performed 10 runs of 20 time units duration of the process (5) starting from $(-2, 0.5)$. The results are presented in both (x, y) and (ξ, y) variables (black trajectories). In the same variables we have simulated from system (2) the "safety trajectory" corresponding to 1000 individuals. The "safety trajectory" was obtained by dichotomy and the observed width $\rho(\varepsilon, k)$ of the funnel is given in Table 2 with corresponding rough evaluations of σ_x and σ_y around the funnel.

- Fig. 10: All the runs are far below the "safety trajectory".
- Fig. 11: All the runs are far above the "safety trajectory" and ultimately reach the vertical line corresponding to 1 individual.

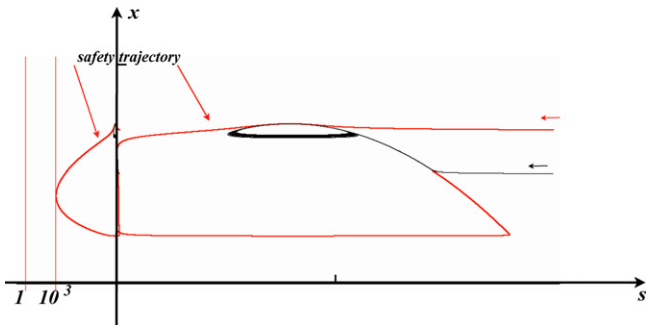

Fig. 10. Ten runs of the process (5) (in black) and the safety trajectory (in red) for $\omega = 10^9$. All trajectories remain below the "safety trajectory". (For interpretation of the references to color in this figure legend, the reader is referred to the web version of this article.)

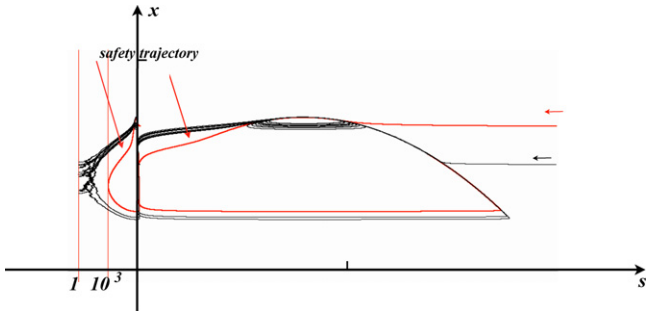

Fig. 11. Ten runs of the diffusion process (5) (in black) and the safety trajectory (in red) for $\omega = 10^6$. All trajectories cross the "safety trajectory". (For interpretation of the references to color in this figure legend, the reader is referred to the web version of this article.)

We observe that when ω decreases the strength of the randomness increases, and at the same time the width of the funnel decreases. These opposite trends are responsible for the sharp transition from extinction to persistence as ω grows from 4.0×10^6 to 2.0×10^7.

6. Methodological comments

6.1. The question of population size

We are used to the fact that continuous differential models work rather well in fluid dynamics and chemical kinetics despite the ultimate discrete nature of fluids. We know that this effectiveness is related to the very large number of atoms in the process. Von Foerster, Lotka, Volterra and others popularized the formalism of chemical kinetics in the domain of population dynamics; they were certainly aware of the limits of such an approach but, in the absence of computers and with a far less developed probability theory, it was nevertheless the right direction.

Now, thanks to computers and probability theory, we have good models for small populations. Unfortunately these discrete models are still expensive in terms of computer time, hence deterministic or diffusion models in continuous variables are still unavoidable. In a diffusion model the size of the population considered is directly

Table 2
Width of the funnel and corresponding σ_x and σ_y.

ω	10^9	10^8	10^7	10^6
$\rho(\varepsilon, k)$	1.2×10^{-3}	9.0×10^{-5}	5.5×10^{-5}	5.3×10^{-5}
$\sigma_x\sqrt{dt}$	4.2×10^{-5}	1.4×10^{-5}	4.2×10^{-5}	1.4×10^{-4}
$\sigma_y\sqrt{dt}$	4.9×10^{-9}	1.4×10^{-7}	4.9×10^{-7}	1.4×10^{-6}

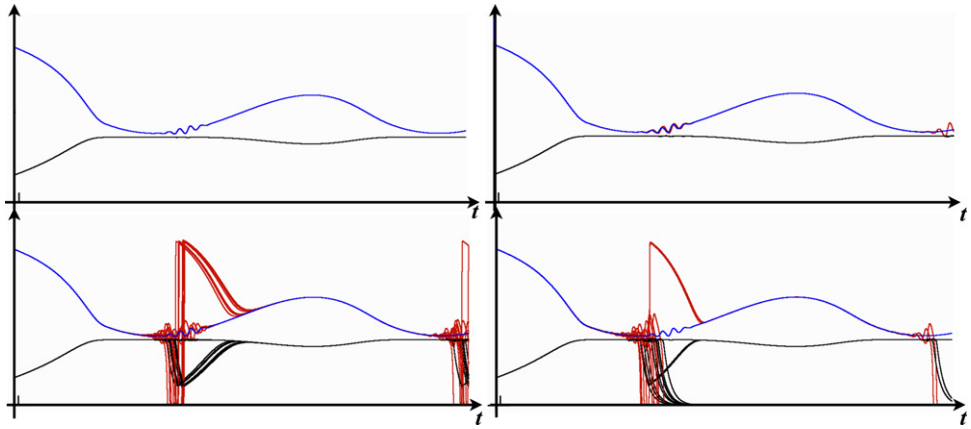

Fig. 12. Comparison of the deterministic model (x in blue, y in black) and the diffusion approximation model (x in red, y in black) for $\omega = 10^{12}$, 10^9 (above left, right) $\omega = 10^8$, 10^7 (below left, right). (For interpretation of the references to color in this figure legend, the reader is referred to the web version of this article.)

related to the "strength" (i.e. standard deviation of the random term).

The predator–prey interaction presented here illustrates the fact that the qualitative behavior of such models may greatly depend on population size even when it is very large.

6.2. About the ubiquity of the phenomenon

The deterministic predator–prey model (2) approximates the dynamics for $\mathbb{E}[x]$ and $\mathbb{E}[y]$ of the birth and death model defined by (3) and of its diffusion approximation (5). This model (2) is the classical deterministic predator–prey model proposed in textbooks as a first improvement of the Lotka–Volterra model. The separation of time scales for prey and predator dynamics introduced by the presence of the parameter ε in the first equation has the following classical explanation. Using a change of unit time, (2) reads:

$$\frac{dx}{d\tau} = [f(x) - \mu(x)y],$$
$$\frac{dy}{d\tau} = \varepsilon(\mu(x) - \delta)y, \quad \varepsilon m = \delta.$$

If we use the same mass unit for x and y then ε is a yield factor. A yield factor of 0.02 is acceptable in ecology (i.e. for 1 kg of cow, 50 kg of dry grass is needed). For bigger ε like 0.1, the sharp transition that we depicted is still present but less spectacular.

As previously noted, we admit that our birth and death model is questionable with respect to its biological signification. There are certainly many different models for individual behavior with the same deterministic equation approximating the mean of the process. Since our point relies on the diffusion approximation for such models, our conclusions are valid as long as such approximation is correct. In the case of birth and death processes, this is valid provided that the number of individuals is greater than 10^3–10^4 which is the case. For more elaborate models, at the individual scale, for instance physiologically structured prey, this point remains to be considered.

6.3. About the existence of "canard" solutions in the model

In a system with two time scales like:

$$\frac{dx}{dt} = \frac{1}{\varepsilon}[f(x,y)], \quad \frac{dy}{dt} = g(x,y)$$

consider the curve Γ defined by the equation $f(x,y) = 0$; this curve splits into two regions:

- the attracting one made of points such that, in their neighborhood, the vector field converges to Γ;
- the repelling one made of points where, in their neighborhood, the vector field diverges from Γ;

and these two regions are separated by equilibria. A *"canard"* solution is a solution of the differential system that follows, for some duration, the attracting part of Γ at a distance of the order of ε and after which, *follows* the repelling part at a distance of order ε. Some "canards" are *robust*, i.e. they persist under small changes in the model, others are not.

The presence of a "safety funnel" like the one described in Section 3 is related to the presence of two "canard solutions" in (2):

- the solution $t \to (x(t) = 0,\ y(t) = y(0)e^{-mt})$ corresponding to the absence of prey;
- the solution following the cubic from the right to the left that has no analytic expression but whose existence can be proved by continuity arguments.

The first "canard" is robust but the second is not. This is the reason why the sharp transition between 4.0×10^6 and 2.0×10^7 individuals occurs for a rather short interval of values of the parameter m. As a consequence, to some extent, our example is exceptional, not "generic". This will be the case in most two dimensional systems, but this does not invalid our point since robust "canard" – different from trivial "canard" corresponding to the absence of some population – are generically present for three dimension and more.

An easy way to understand this is to imagine that our parameter m is of the form:

$$m(t) = a + b\ \cos(rt)$$

which mimics, for instance, some seasonal dependence of the mortality rate. This non autonomous system can be considered as a three dimensional system, and we see that the "canard" value for m is crossed periodically. We have done a simulation in the case of:

$$m(t) = 0.6645 - 0.047\,(1 - \cos(0.1\,t))$$

and the results are shown in Fig. 12. For $\omega = 10^{12}$ we observe no difference between the deterministic model (x in blue, y in black) and the diffusion approximation (x in red, y in black); for $\omega = 10^9$ we observe a very slight deviation between the red and blue curves; for $\omega = 10^8$ we observe a large difference with now a mixed mode oscillation in the diffusion process; for $\omega = 10^7$ the mixed mode oscillation leads to extinction.

6.4. About the inadequacy of deterministic models in continuous variables

In population dynamics there is agreement that deterministic models are simply crude approximations of reality. Only individually based models, stochastic by essence, can correctly represent the evolution of real ecosystems. The example presented here is just one more argument against the danger of using deterministic differential equations without care.

But it is by no means an argument against the study of continuous deterministic differential models of populations dynamics!

Actually there are many good reasons for continuing to explore systems of ordinary differential equations:

- Some models are mathematically appealing. For instance the proof of the exclusion principle for the most general model of competition in the chemostat (Smith and Waltman, 1995), despite its poor ecological contents, remains an interesting mathematical challenge for mathematicians.
- More interesting is the use of easily tractable mathematical models to formalize ecological issues and to clarify the discussion. An interesting example of this use of differential equations is given by the discussion on "ratio dependent" models initiated by Arditi and Ginzburg (1989).
- In our example, the understanding of the diffusion model, relies on very particular and recently discovered properties of *deterministic* differential systems, known as "canard solutions", see Appendix B.

In addition, far from being against the use of deterministic differential systems, our work supports the importance of a thorough understanding of the properties of ordinary differential systems in population dynamics. In particular it shows that the classical deterministic definition of persistence:

$$\limsup x(t) = \alpha > 0$$

must be enriched by some consideration of the "size" of α.

6.5. About computer simulations in dynamic population modeling

One may ask to what extent this phenomenon of sharp transition is just a computer artifact. This is not the case since our mathematical explanation of the phenomenon which is independent of any computer simulation, shows us that simulations of the same model on a different computer with a different computer language will give qualitatively the same.

There is no doubt that our mathematical understanding of the phenomena outlined in the present article will considerably increase in the future. But this will require highly sophisticated mathematics and time. Unfortunately, in the mean time, biologists will use models and computer simulations that are not completely safe. It urges us to provide them with computer routines that are safe from artifacts associated with the representation of a finite number of individuals by *real numbers*. Considering present mathematical knowledge, this certainly can be done in a comparatively short time but it will require many people working on the development of safe computer software. This has been done in the past for the needs of industry (for instance digital wind tunnels), medicine (medical imaging); this also could be done for population dynamics, but it is dependent on decisions at the level of scientific policymaking.

7. Conclusion

Scientists are now much familiar with the phenomenon of "sensitivity to initial conditions" which, in some deterministic dynamical systems, is the cause of unpredictable long range behaviors. The same phenomenon occurs in some deterministic differential equations modeling the dynamic behavior of populations where very small differences in the initial condition (or along the trajectory) will make the future values of some variables very small or not. This is the reason why, in the modeling of population dynamics, it is well-advised to add a small noise to the deterministic process; indeed it does not cost too much computer time and may detect this kind of phenomenon. But we have shown that the result may depend strongly on the intensity of the noise. In addition, when no accurate estimation of the noise intensity is available, it would be prudent to vary the noise intensity and to make sure that the behavior of the system is not strongly affected.

Acknowledgements

Since the publication of Lobry and Sari (2009), on which the "deterministic part" of the present work is based, we have greatly benefited from discussions with T. Sari, J. Harmand and A. Rapaport from the Modemic Team (http://team.inria.fr/modemic/). We warmly thank them.

We acknowledge the financial support of the French National Research Agency (ANR) within the SYSCOMM project DISCO ANR-09-SYSC-003.

We thank an anonymous referee for very valuable comments which helped us to improve our paper.

Appendix A. Approximation by a diffusion process

Consider the process defined by (3). Since Z follows an exponential distribution law of parameter λ its expectation is $\frac{1}{\lambda}$ and the number N_b of events during the duration dt is approximately:

$$N_b \approx \frac{dt}{(1/\lambda)} = dt\,\lambda = dt\,\frac{\omega}{\varepsilon}\,(f(x) + \mu(x)y).$$

We consider N_b as deterministic. If dt is small, the variables $x(t)$ and $y(t)$ are approximately constant. Denote by X_i the random variable which is equal to 1 if at the ith event a predation occurs; one has:

$$\mathbb{P}(X_i = +1) = \frac{\mu(x(t))y(t)}{f(x(t)) + \mu(x(t))y(t)},$$
$$\mathbb{P}(X_i = 0) = \frac{f(x(t))}{f(x(t)) + \mu(x(t))y(t)}.$$

The number of predations during $[t, t+dt]$ is approximately $\sum_{i=1}^{N_b} X_i$ and the number of births is by the way of $N_b - \sum_{i=1}^{N_b} X_i$ and the increment of the number of individuals is $N_b - 2\sum_{i=1}^{N_b} X_i$.

One has:

$$\mathbb{E}[X_i] = \frac{\mu(x(t))y(t)}{f(x(t)) + \mu(x(t))y(t)},$$

$$\mathbb{E}[\sum_{i=1}^{N_b} X_i] = dt\frac{\omega}{\varepsilon}(f(x(t)) + \mu(x(t))y(t))\frac{\mu(x(t))y(t)}{f(x(t)) + \mu(x(t))y(t)}$$
$$= dt\frac{\omega}{\varepsilon}\mu(x(t))y(t),$$

$$\sigma^2(X_i) = \frac{f(x(t))\mu(x(t))y(t)}{(f(x(t)) + \mu(x(t))y(t))^2},$$

$$\sigma^2(\sum_{i=1}^{N_b} X_i) = dt\frac{\omega}{\varepsilon}(f(x(t)) + \mu(x(t))y(t))\frac{f(x(t))\mu(x(t))y(t)}{(f(x(t)) + \mu(x(t))y(t))^2},$$

$$\sigma^2(\sum_{i=1}^{N_b} X_i) = dt\frac{\omega}{\varepsilon}\frac{f(x(t))\mu(x(t))y(t)}{(f(x(t)) + \mu(x(t))y(t))}.$$

From the central limit theorem we can approximate the sum by a Gaussian random variable and we write:

$$\sum_{i=1}^{N_b} X_i \approx dt\,\frac{\omega}{\varepsilon}\,\mu(x(t))y(t) + \sqrt{dt\frac{\omega}{\varepsilon}\frac{f(x(t))\mu(x(t))y(t)}{(f(x(t)) + \mu(x(t))y(t))}}W_t$$

where W_t is a Gaussian variable of mean 0 mean and standard deviation 1.

Since the variable x is the number of individuals divided by ω; the increment of x is given by:

$$x(t+dt) - x(t) = \frac{1}{\omega}(N_b - 2\sum_{i=1}^{N_b} X_i) \approx \frac{1}{\omega}\left\{N_b - 2\left\{dt\frac{\omega}{\varepsilon}\mu(x(t))y(t)\right.\right.$$
$$\left.\left. + \sqrt{dt\frac{\omega}{\varepsilon}\frac{f(x(t))\mu(x(t))y(t)}{(f(x(t)) + \mu(x(t))y(t))}}W_t\right\}\right\}$$

and replacing by the value of N_b one gets:

$$x(t+dt) - x(t) \approx dt\frac{1}{\varepsilon}[f(x(t)) - \mu(x(t))y(t)]$$
$$- \sqrt{dt\frac{4}{\omega\varepsilon}\frac{f(x(t))\mu(x(t))y(t)}{(f(x(t)) + \mu(x(t))y(t))}}W_t.$$

Let us now compute the increment of y. According to (3c) we have:

$$y(t+dt) = y(t) - dt\,m\,y(t) + \varepsilon\{\text{number of prey death during} \times [t, t+dt]\}$$

which, according to the previous notations is:

$$y(t+dt) - y(t) = -dt\,my(t) + \frac{\varepsilon}{\omega}\sum_{i=1}^{N_b} X_i$$

and introducing W_t one gets:

$$y(t+dt) - y(t) \approx dt\,[\mu(x(t)) - m]y(t)$$
$$+ \sqrt{dt\,\frac{\varepsilon}{\omega}\frac{f(x(t))\mu(x(t))y(t)}{(f(x(t)) + \mu(x(t))y(t))}}W_t.$$

Appendix B. "Canard solutions"

As already stated, "canards" are specific solutions in singular perturbations of differential equations. They were discovered in 1981 by a group of students of G. Reeb (Benoıt et al., 1981). The word "canard" comes from the fact that the first discovered "canard solution" was responsible for the existence of a limit cycle in the Van der Pol equation and the shape of this limit cycle looked like a caricature of a duck: "canard" is the French word for duck. They studied "canard solutions" within the framework of Nonstandard Analysis, which is a very suitable framework for modeling since it is a simple formal language where the use of infinitesimals, in the sense which physicists use this term, is mathematically rigorous; see Lobry and Sari (2007) for nonstandard analysis applied to real word questions. Since the tradition among mathematicians is not to use nonstandard analysis, "canard solutions" are now also studied by numerous mathematicians within the classical framework of *matched asymptotic expansion* or of the *geometric singular perturbation theory*. The reader who wants to know more about "canard solutions" and related subjects is encouraged to read Wechselberger (2007) which is a *scholarpedia* article and is available on the web. It is a succinct and very nice introduction.

The reference Desroches et al. (2012) is a thorough survey, for mathematically trained people, about our present understanding of "canards" with a focus on numerical questions. The question of considering the presence of noise in singularly perturbed systems has long been addressed. We refer to the recent article Berglund et al. (2012) devoted to the question of the consequence of noisy environments on "canard solutions" and its bibliography. In particular the results contained in this article allow us to give asymptotic evaluations of the width of the "safety funnel" and of many other quantities of interest. However, their mathematical sophistication is out of the scope of the present work.

Appendix C. Exponentially small values

Let us write explicitly system (2) as:

$$\begin{cases} \dfrac{dx}{dt} = \dfrac{1}{\varepsilon}\left[0.5x(2-x) - \dfrac{x}{0.4+x}y\right], \\ \dfrac{dy}{dt} = \left(\dfrac{x}{0.4+x} - m\right)y. \end{cases} \tag{C.1}$$

In the variables (ξ, y) the system writes:

$$\begin{cases} \dfrac{d\xi}{dt} = 0.5(2 - \exp(\xi/\varepsilon)) - \dfrac{1}{0.4+\exp(\xi/\varepsilon)}y, \\ \dfrac{dy}{dt} = \left(\dfrac{\exp(\xi/\varepsilon)}{0.4+\exp(\xi/\varepsilon)} - m\right)y. \end{cases}$$

When $\xi < 0$, which is the case since we are interested by $x < 1$, and when $|\xi| \gg \varepsilon$ we have $\exp(\xi/\varepsilon) \ll 1$ and thus we can neglect this term and approximate the system by:

$$\begin{cases} \dfrac{dx}{dt} = [1 - 2.5y], \\ \dfrac{dy}{dt} = -my. \end{cases} \tag{C.2}$$

Explicit solutions of this last system are easily computed from which one can compute an estimation for the minimum of ξ^*. For instance, if we take as initial condition $(\xi_0, y_0) = (-0.1, 0.9)$, which corresponds to trajectory No. 1 in Fig. 7, then this minimum is approximatively 1, as seen in Fig. 7. Moreover, the minimum x^* is of the order of:

$$x^* = e^{\xi^*/0.02} \approx e^{-40} \approx 10^{-17}.$$

The minimum depends greatly on the value of y_0: The largest is y_0 the smallest is the minimum. This explain why in Fig. 8 the minimum corresponding to trajectory 6 is much bigger.

Appendix D. Numerical simulations

We have not made use of a numerical solver. A specific software was written in order to be sure that there were no artifacts caused by the erroneous use of some sophisticated numerical scheme. Trajectories of the differential equations (2) are obtained using the Euler scheme defined by (6). We prefer this scheme to more sophisticated ones since it is the exact recurrence scheme which approximates for $\mathbb{E}[x(t)]$ and $\mathbb{E}[y(t)]$ of the diffusion process (5).

We fixed $dt = 10^{-4}$ since we observed that for this value the solutions of (6) are indistinguishable from those with $dt = 10^{-5}$.

The birth and death process defined by (3) takes too long to be simulated when λ is very large, in the case of our computer $\omega > 10^6$. This is why we used a diffusion approximation which is a perfect approximation for large values. Since we were mainly interested in the funnel phenomenon associated to "canard" it was not necessary to switch to the true birth and death process for small values of λ. But if one is interested in such figures as the mean of the extinction time, it would be better to switch to some suitable jump process.

References

Arditi, R., Ginzburg, L.R., 1989. Coupling in predator–prey dynamics: ratio-dependency. Journal of Theoretical Biology 139, 311–326.

Bartlett, M.S., 1957. On theoretical models for competitive and predatory biological systems. Biometrika 44 (1/2), 27–42.

Benoıt, E., Callot, J.L., Diener, F., Diener, M., 1981. Chasse au canard. Collectanea Mathematica 31–32 (1–3), 37–119.

Berglund, N., Gentz, B., Kuehn, C., 2012. Hunting French ducks in a noisy environment. Journal of Differential Equations 252 (9), 4786–4841.

Desroches, M., Guckenheimer, J., Krauskopf, B., Kuehn, C., Osinga, H.M., Wechselberger, M., 2012. Mixed-mode oscillations with multiple time scales. SIAM Review 54 (2), 211–288.

Feller, W., 1939. Die Grundlagen der Volterraschen Theorie des Kampfes ums Dasein in wahrscheinlichkeitstheoretischer Behandlung. Acta Biotheoretica 5, 11–40.

Gard, T.C., Kannan, D., 1976. On a stochastic differential equation modeling of prey–predator evolution. Journal of Applied Probability 13 (3), 429–443.

Gillespie, D., 1977. Exact stochastic simulation of coupled chemical reactions. Journal of Physical Chemistry 81 (25), 2340–2361.

Leslie, P.H., 1958. A stochastic model for studying the properties of certain biological systems by numerical methods. Biometrika 45 (1/2), 16–31.

Lobry, C., Sari, T., 2007. Nonstandard analysis and representation of real world. International Journal on Control 80 (3), 171–193.

Lobry, C., Sari, T., 2009. La modélisation de la persistance en écologie. In: First Congress of the Moroccan Society of Applied Mathematics, February 6–8, 2008, Rabat.

Mollison, D., 1991. Dependence of epidemic and population velocities on basic parameters. Mathematical Biosciences 107, 255–287.

Murray, J.D., Stanley, E.A., Brown, D.L., 1986. On the spatial spread of rabies among foxes. Proceeding of the Royal Society of London, Series B: Biological Sciences 229 (1255), 111–150.

Smith, H.L., Waltman, P.E., 1995. The Theory of the Chemostat: Dynamics of Microbial Competition. Cambridge University Press.

Turner, A.G., 2007. Convergence of Markov processes near saddle fixed points. The Annals of Probability 35 (3), 1141–1171.

Wechselberger, M., 2007. Canards. Scholarpedia 2 (4), 1356, http://www.scholarpedia.org/article/Canards.